The distance to the galactic centre derived from RR Lyrae variables, the distribution of these variables in the galaxy's inner region and halo, and a rediscussion of the galactic rotation constants

Oort, J.H.; Plaut, L.

Astron. & Astrophys. 41, 71–86 (1975)

The Distance to the Galactic Centre Derived from RR Lyrae Variables, the Distribution of these Variables in the Galaxy's Inner Region and Halo, and a Rediscussion of the Galactic Rotation Constants

J. H. Oort
Sterrewacht, Leiden

L. Plaut
Sterrenkundig Laboratorium "Kapteyn", Groningen

Received March 28, 1975

Summary. The results of recent surveys of faint RR Lyrae variables in fields near the galactic centre are discussed. The density distributions show sharp maxima, and half-widths between 2 and 3 kpc. They indicate that the distance to the centre is 8.7 kpc, with a mean error of about ± 0.6 kpc, the largest uncertainty being in the assumed absolute magnitude. The distance can be satisfactorily reconciled with the data on galactic rotation.

The density distribution of the variables has been determined up to a distance R of about 5 kpc from the centre. Except in the layer within 1.0 kpc from the galactic plane it seems to be almost spherical; the axial ratio of the equidensity surfaces is unlikely to be smaller than about 0.8. The density varies as R^{-3}, and is about 260 per kpc^3 at $R = 1.5$. Within 1 kpc from the plane the density is higher than would correspond to these numbers, but the data are insufficient for an unambiguous derivation of the distribution in this layer. There may be an extra concentration near the centre, with a density of about 12000 per kpc^3 at $R = 0.6$ (the smallest distance reached by the available data). The R^{-3} variation for the density corresponds to a Maxwellian velocity distribution with a dispersion of 125 km/s in one co-ordinate.

Between 6° and 16° latitude the variables with high and low metal-abundance parameters as inferred from their periods and amplitudes show practically identical density distributions.

In all fields the average absorption in front of the distant variables is about 4 times less than that which has been inferred from galaxy counts.

Key words: galactic centre — rotation constants — RR Lyrae variables — galactic structure

1. General

Probably the most reliable way in which the distance of the galactic centre can be determined is through the study of faint RR Lyrae variables. In the following a discussion is given of their space distribution as found from the Palomar-Groningen variable star survey (Plaut, Papers I–VI, cf. under References). A provisional discussion of the density distribution and the distance to the centre was given in Paper IV (it should be mentioned that the factors used in that paper to convert r_{max} to R_0 for different axial ratios of the density distribution were erroneous). The fields in the central region had been selected by Baade and Plaut for optimum transparency and lack of obvious absorption features. At positive latitudes it did not prove possible to comply satisfactorily with the latter condition; the field finally selected (centered at $l = 4°$, $b = +12°$) proved to have a number of extensive dark regions in its lower-latitude half. We therefore had to reject this half of the field in the final discussion. The data of the Palomar-Groningen survey were supplemented by those of Baade's pioneer investigation of the region around NGC 6522, rediscussed so as to make them approximately homogeneous with those of the other fields (Plaut, 1973a). Data on two other transparent low-latitude fields near the centre were obtained by Oosterhoff *et al.* (1967, 1968) from plates taken by Thackeray with the Radcliffe 74-inch reflector. These fields, Sgr I at $l = 1°.4$, $b = -2°.6$, and Sgr II at $l = 4°.2$, $b = -5°.1$, may yield valuable additional information as soon as absorption measures have been made.

The plates for the Palomar-Groningen survey were all taken with the 48-inch Schmidt telescope. They were taken in the photographic as well as the photovisual region. The number of plates in each field was sufficient

Table 1. Data about the fields

Field	l	b	Area (square degrees)	n	σ (per s.d.)	A_{pg}	$\langle A_{pg}\rangle$	r_{max} (kpc)	Half width (kpc)	Ref.
NGC 6522	1.0	− 3.9	0.220	110	336	1.80	1.80	9.3	1.5	Plaut (1973a)
3 low	0	− 8	19.5	379	19.4	$-0.08+0.116/\sin b$	0.73	8.1	3.1	Papers IV and V
2 low	4	+10	21.0	238	11.3	$-0.08+0.232/\sin b$	1.24			Papers II and III
3 high	0	−12	22.7	261	11.5	$-0.08+0.116/\sin b$	0.49	7.8	2.3	Papers IV and V
2 high	4	+14	21.1	180	8.5	$-0.08+0.232/\sin b$	0.85	8.8	3.4	Papers II and III
1	0	+29	42.9	50	1.17	0.60	0.60	5.9		Paper I

to obtain reliable periods and light-curves, and to determine the measure of completeness of the discoveries. The limiting magnitude is between 19.5 and 20.0.

Van den Bergh (private communication) has drawn attention to the fact that the photographic images of a large fraction of the faint RR Lyrae stars show interference by images of neighbouring stars. It is scarcely possible to take exactly account of these interferences. They will have different influence in the case of photoelectric observations, which use diaphragms of constant size for all stars, and at iris photometry on photographic plates. Hence, systematic errors may be introduced; however, precautions were taken as far as possible. Van den Bergh (1971) also shows that systematic differences between two photoelectric magnitude scales and between photoelectric and photographic scales will arise from a different choice in the sky background. Two possibilities exist: first to take the background at positions selected at random near each star, second at pre-selected star-free sky patches. As van den Bergh (loc. cit.) mentions "the first procedure has the advantage that it is completely free from any systematic bias. It has the disadvantage that it increases the uncertainty in the true background corrections for individual stars". In the measurements on which the present investigation is based, the first procedure was used; however, clearly visible background sources were, of course, excluded from the sky measurements.

Recent photoelectric observations of the standard stars in fields 1, 2 and 3, and also observations of several RR Lyraes confirm the magnitude scale and zero points as used in the original computations (cf. Paper VI; Plaut, 1973b).

The fields are listed in Table 1, in order of increasing galactic latitude. The first column gives the name by which the field will be referred to. Fields 2 and 3 of the survey were divided into a lower- and higher-galactic latitude half. The second column gives the galactic coordinates of the centres. The following columns contain the surface area in square degrees, the number of RR Lyrae variables used in the analysis, and their surface density per square degree, σ. The column A_{pg} gives the assumed photographic absorption and its average for the field. References are given in the last column.

2. Adopted Mean Absolute Magnitude

The distances in the present paper were derived on the assumption that $\bar{M}_{pg} = +0.70$, where $\bar{M}_{pg}$ is the mean of the maximum and minimum magnitudes. This assumption is consistent with recent determinations of the absolute magnitude of RR Lyrae stars, as indicated in Table 2. The values of $\langle M_V\rangle$ refer to the magnitude at average intensity. For an average light-curve of a variable of type a and b we find $\bar{M} = \langle M\rangle - 0.14$. The intrinsic colour index $\langle B-V\rangle$ at average intensity is about 0.21 mag (see the following section). The corresponding values for $\bar{M}_{pg}$ are given in the third column. The first three determinations are based on different proper motion data for the brighter field RR Lyrae variables. The last two are independent. In computing the total average we have given half weight to Hemenway's result because of its larger mean error, and unit weight to each of the others. These weights are necessarily somewhat arbitrary. We then obtain $\bar{M} = +0.70$. The uncertainty might be about ± 0.15.

In Papers I–VI and Plaut (1973a) a round value of $+1.00$, close to van Herk's result, had been used for $\bar{M}_{pg}$. A mean absolute magnitude of $+0.70$ now appears preferable.

Table 2. Absolute magnitude of RRa variables

		$\bar{M}_{pg}$	w
Van Herk (1965)	$\bar{M}_{pg} = +0.87 \pm 0.22$	+0.87	1
Woolley (1971)	$\langle M_V\rangle = 0.0 - 2.5 \log P$	+0.77	1
Hemenway (1971), for RRa stars	$\langle M_V\rangle = +0.5 \pm 0.4$	+0.57	½
Sandage (1970), from globular clusters	$\langle M_V\rangle = +0.6 \pm 0.2$	+0.67	1
Graham (1973), from Magellanic Clouds	$\langle M_V\rangle = +0.5$ (LMC) $\langle M_V\rangle = +0.45$ (SMC)	+0.55	1

3. Interstellar Absorption

The corrections for interstellar absorption indicated in Table 1 were derived in two independent ways: firstly from the colours of the variables derived from the photographic and photovisual magnitudes, calibrated with the aid of the comparison stars whose magnitudes were determined by photographic transfers from standard stars (cf. Papers I, II and IV), and secondly from photoelectric B and V magnitudes determined for 20 variables in fields 1, 2 and 3. These latter have been discussed in Paper VI. Intrinsic colours were derived from observations by Fitch *et al.* (1966); they depend upon period and amplitude in the way given in Paper VI. The average intrinsic colour at minimum for the stars used is $+0^{m}.38$. This may be compared with the observations of Southern variables by Clube *et al.* (1969); from the seven variables at latitudes larger than 45° (their Fig. 9) and the corresponding colour excess as given in their Fig. 10 we obtain $+0^{m}.35$ for the average intrinsic colour at minimum, in good agreement with the above value from Fitch *et al.* As the average range in colour is $0^{m}.31$, the intrinsic colour for the average between maximum and minimum becomes $+0^{m}.21$.

This value has been used for the determination of the photographic colour excesses. The comparison between the photoelectric and photographic colour-excesses shows no significant systematic difference (cf. Fig. 1 of Paper VI). It is to be noted that the values used in the present article are $0^{m}.05$ smaller than indicated in Paper VI, because a rediscussion of the intrinsic colours gave a $0^{m}.05$ higher value (viz. $+0^{m}.21$) than was used in the earlier articles. The colour excesses used in the present analysis for fields 3 and 2 are indicated by the lower of the broken lines in the figure mentioned; the photoelectric data are indicated by dots. Both must be decreased by $0^{m}.05$, as mentioned above. The uncertain low-latitude half of field 2 has been discarded, as has been explained above. It should be stressed that in view of the great spread in the absorptions for individual stars the number of variables for which photoelectric light-curves were determined is still too small to permit a sufficiently reliable comparison. The absorption has been assumed to occur near-by, and therefore to be the same for bright and faint variables. It is conceivable that there would also be some absorption in the central bulge itself. However, the present observations show no evidence for an appreciable change of the mean colours with distance. In field 3 an indication was found of a change of $+0.07$ per magnitude (Paper IV). If real, this would make the half-width of the density distribution about 7% smaller. In fields 1 and 2 there was no indication of a significant systematic change in colour. The absorption for the field around NGC 6522 was taken from a recent investigation of van den Bergh (1971).

We want to draw attention to a striking discrepancy between our absorptions and the much larger values indicated by the near absence of faint galaxies in these regions. The galaxy counts by Shane and Wirtanen (1967) give approximately 3 galaxies per square degree in "field 2 high", and about 10 in field 1. As their average number for an absorption-free field is 90, these data would indicate absorptions of $3^{m}.0$ and $2^{m}.0$ respectively, whereas we found $0^{m}.8$ and $0^{m}.6$. Field 3 lies below the declination limit of Shane and Wirtanen's survey, but is situated well within the "zone of avoidance" outlined by Hubble (1934); the absorption inferred from the galaxy counts is therefore probably of the same order as in "field 2 high", and again much larger than the values of $0^{m}.7$ and $0^{m}.5$ found from the RR Lyrae variables.

Though it has been suggested that the straightforward transformation of galaxy counts into absorptions may give too high values for the latter, it is difficult to understand how absorptions as low as $0^{m}.5$ to $0^{m}.8$ could cause an almost complete absence of galaxies. While our absorptions are rather uncertain it appears out of the question that they could have been underestimated by the factors of 3 or 4 that would be required to reconcile them with the evidence of the nebula counts. Moreover, a substantial increase of the absorptions would lead to an inadmissably small value for the distance to the galactic centre. We have been unable to find a satisfactory explanation of the discrepancy.

Since the above was written Dr. Wesselink pointed out to us that in his opinion the absorption inferred from the galaxy counts might well be wrong by factors of the size just mentioned, due to the very large effect which crowding of stellar images may have on surveys for faint nebulae. He was struck by this in his attempt to determine the absorption by the Small Magellanic Cloud from galaxy counts (Wesselink, 1961). Wesselink's low value for the absorption in this Cloud has recently been confirmed by Hodge (1974). It should be mentioned that colour excesses of individual objects at various galactic latitudes also indicate absorptions which are lower than those found from the galaxy counts. As an example we refer to a recent study by Knapp and Kerr (1974) of the correlation between the reddening of globular clusters and the hydrogen column density in front of them.

On the other hand Holmberg (1974) has recently collected weighty evidence for the existence of considerable absorption in intermediate and high latitudes. From a careful discussion of all available data he concludes that the average colour excess in $B-V$ can be well represented by $(0^{m}.054 \pm 0^{m}.004)\,\mathrm{cosec}\,b$, which, with a normal ratio of photographic to $B-V$ absorption, corresponds with $0^{m}.22\,\mathrm{cosec}\,b$ photographic extinction.

4. The Incompleteness of the Discoveries

A special effort has been made to determine what fraction of the variables has remained undiscovered after the blinking of the ten plate pairs used for the search in each field. For a detailed discussion the reader is referred to Paper I. The incompleteness factors f were determined as a function of apparent magnitude and amplitude. They were later re-examined, and confirmed (Paper VI). The new values of $1/f$ for field 3 are shown in Table 3 together with those found in Paper I for fields 1 and 2. The two sets differ very little. The density distributions given in the present article as well as in preceding papers refer exclusively to variables of types a and b, and with amplitudes of $0^m.50$ and larger, for which the incompleteness is never very large. No corrections for incompleteness were applied for Baade's field at $b = -3°.9$.

For the present investigation average factors were derived for various magnitudes (bottom line of Table 3), and final values were read from a smooth curve giving the relation between f and $\bar{m}$ (Fig. 1). It may be noted that the factors are small and well-determined for the range of magnitudes with which we are concerned. In our fields the maxima of the density all lie between $15^m.9$ and $16^m.5$, and the significant parts of the distributions do not extend further than $1^m.5$ beyond the maxima.

5. Distance Distribution and Correction for Random Errors in the Distances

The dots in Fig. 2 show the counts of the a and b variables with amplitudes larger than $0^m.49$ in intervals of 0.25 in $\bar{m}_{pg}$. Mean errors are indicated by the vertical lines on either side of the observed points. A smooth curve has been drawn through these points. Corresponding values of $\log r$, based on an assumed absolute magnitude $\bar{M}_{pg}$ of $+0.70$ and absorptions as given in Table 1 are also indicated.

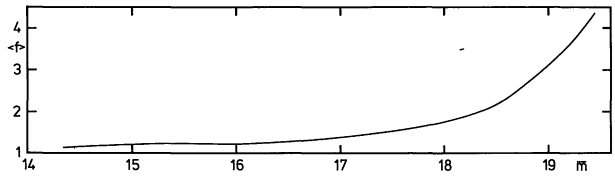

Fig. 1. Average incompleteness factors f as a function of mean magnitude

The true distribution of $\log r$ will differ systematically from those given in Fig. 2, due to the accidental errors in the magnitudes, the dispersion in the average absolute magnitude, and the differences between the absorptions for individual stars and the average absorption values used in each field. The mean error in the average apparent magnitudes of the variable stars was estimated to be about $\pm 0^m.1$. The dispersion in $\bar{M}$ may be about $\pm 0^m.2$ (see, for instance, Graham, 1973). We have been unable to make a useful estimate of the dispersion in the absorption. We tried to determine this from the spread of the individual colour excesses in Fig. 1 of Paper VI. For field 3 and field 2 "high" this gave $\pm 0^m.5$. The distribution curves in Fig. 2 are, however, too narrow to allow such large errors in the distance moduli. Rough calculations show that in order to obtain plausible distance distributions the mean error should not be larger than about $\pm 0^m.3$. It appears, therefore, that the deviations of the photoelectric colour excesses should be largely ascribed to errors in the observations rather than to irregularities in the absorption. This conclusion is supported by the lack of correlation between the colour excess of a variable and the star counts in its vicinity (Paper VI, p. 355). In the final reductions a total mean error of $\pm 0^m.26$ has generally been used. The way in which the results are affected by using different mean errors is investigated in Section 7.

A rough idea of the effect of the correction for random errors may be seen in the dashed curves in Fig. 2. These were obtained from the full-drawn smooth curves through the observed points by applying an approximate correction in the form first used by Eddington

Table 3. Average chance of discovery, $1/f$, after blinking ten pairs of plates, as a function of mean magnitude and amplitude, for fields 1 and 3, respectively. The frequency distribution of the amplitudes is given under ϕ. The bottom line shows the mean values of f for all fields, weighted with ϕ

A	ϕ	$\bar{m} < 15.0$		$\bar{m}$ 15.0–16.0		$\bar{m}$ 16.0–17.0		$\bar{m}$ 17.0–18.0		$\bar{m}$ 18.0–19.0		$\bar{m} > 19.0$	
0.60	0.03	0.575	0.519	0.426	0.409	0.285	0.298	0.207	0.190	0.069	0.087	0.000	0.007
0.80	0.08	0.725	0.673	0.594	0.579	0.484	0.483	0.402	0.379	0.224	0.246	0.069	0.093
1.00	0.12	0.821	0.786	0.721	0.719	0.632	0.642	0.565	0.550	0.389	0.385	0.141	0.133
1.25	0.29	0.906	0.884	0.843	0.838	0.779	0.787	0.728	0.727	0.575	0.574	0.247	0.282
1.50	0.28	0.951	0.932	0.910	0.903	0.869	0.870	0.831	0.828	0.702	0.698	0.342	0.380
1.75		0.974	0.963	0.949	0.944	0.922	0.923	0.898	0.894	0.793	0.791	0.432	0.482
2.00	0.21	0.986		0.970		0.953		0.936		0.854		0.521	
3.00		0.998		0.995		0.990		0.987		0.951		0.746	
4.00		0.999		0.998		0.997		0.996		0.976		0.857	
$\langle f \rangle$		1.14		1.23		1.36		1.52		2.18		4.22	

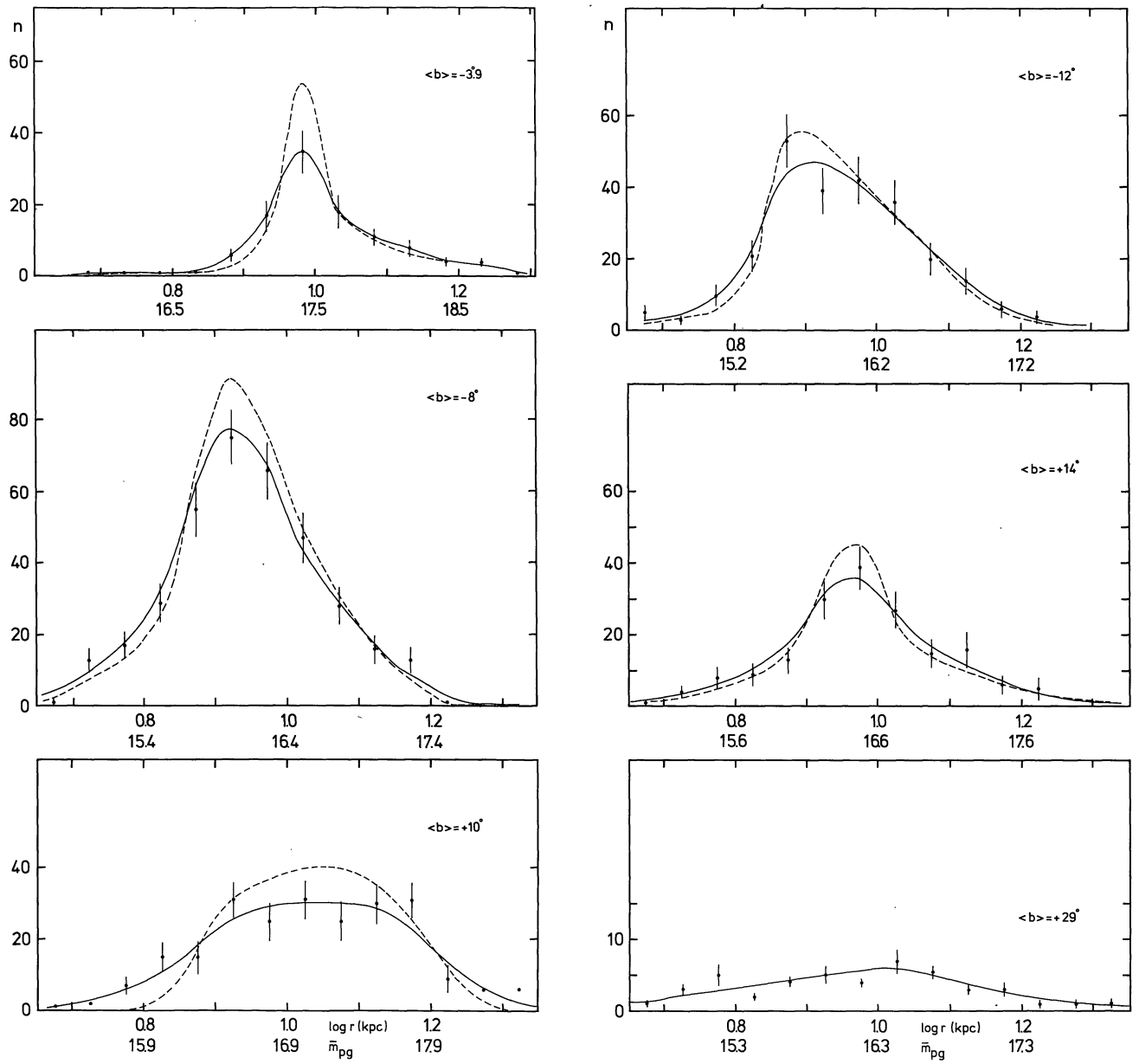

Fig. 2. Numbers of RR Lyrae variables per 0.25 interval in magnitude. Corresponding values of log$r$ (r = distance in kpc) are also indicated. Vertical bars indicate mean errors. Full-drawn curves are smooth representations of the counts. Dashed curves were obtained by correcting the observed data for the effects of random errors

(1913). It is given by the expression

$$\text{correction} = -\left(\frac{0.70 \times \text{mean error}}{\text{tabular interval}}\right)^2 \times \text{tabular second difference.}$$

In our case the tabular interval in log$r$ is 0.05, and the mean error in log$r$ $\pm 0.052(0.26/5)$, as just estimated, except for field 2 "high" where it was taken ± 0.060. The formula is applicable only in case the errors have a gaussian distribution. The actual distribution of the absorptions may well deviate considerably from this.

Table 1 gives the distance r_{max} around which the density distributions are roughly symmetrical, and the widths of the corrected curves at a density equal to half the maximum density. We wish to draw attention in particular to the narrowness of the density distributions. This narrowness would have been even more extreme had we applied corrections based on the error dispersion of about $\pm 0^m.5$ estimated above from the observed dispersion in the absorptions. In fact, application of such a large correction would have led to impossible results.

A more adequate discussion of the distance distributions will be given in Section 7.

Figure 2 shows that the curve for the discarded "field 2 low" is entirely different from that of the other low-

latitude fields. This is doubtlessly due to the large and irregular absorption in this field noted in the beginning of our article (cf. also Paper II).

6. Different Populations

It might be that the variables in the central region differ systematically from those used for the determination of the mean absolute magnitude. In order to check this we have divided the variables in two groups according to their metal content, using the period and amplitude as an indicator of the metal-content parameter ΔS. The division was made by means of the relation

$$P = 0.720 - 0.149\,A\,,$$

where P is the period corresponding with $\Delta S = 5$, and A is the photographic amplitude (Paper VI). The result is shown in Fig. 3 for the fields at $b = -8°$ and $+14°$, respectively. Ordinates are logarithms of the density per kpc^3. There appears to be no significant difference between the two categories. This curious similarity of the distributions of two classes of stars which have such very different velocity dispersions in the vicinity of the Sun is confirmed by their distribution in latitude. Table 4 gives the numbers of variables which according to the above relation would have high metal content (short periods) and those with longer periods (and presumably lower metal content). The table indicates that there is practically no decrease in the proportion of the shorter-period stars between 8° and 14° latitude. Only the field at 29° seems to show some deficit of short-periods; the reverse may hold for Baade's field at $b = -3°.9$, but periods as well as amplitudes are uncertain in that field.

Table 4. Numbers of variables with relatively high ("ΔS" < 5) and relatively low metal content in the various fields

b	"ΔS" < 5	"ΔS" > 5
− 3°.9	42	17
− 8	166	176
+10	113	120
−12	107	127
+14	80	101
+29	15	34

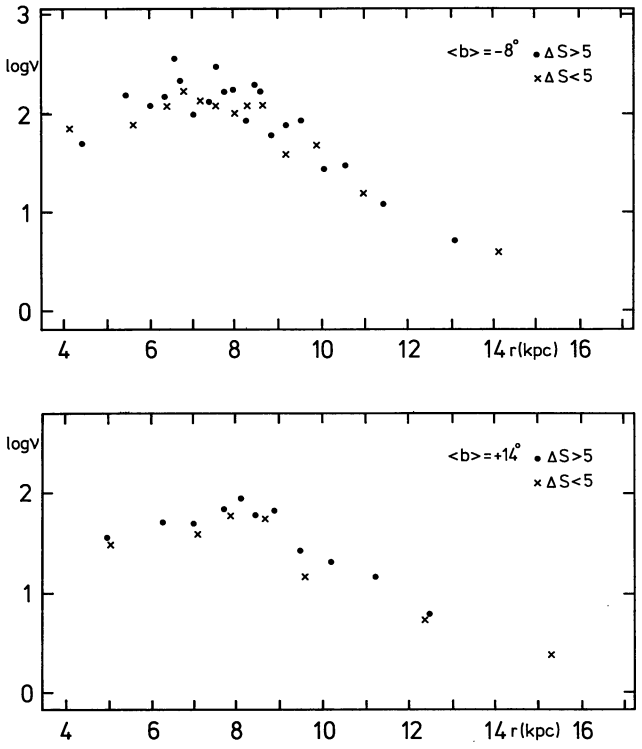

Fig. 3. Comparison of log ν-distributions for variables with high ($\Delta S < 5$) and low metal content ($\Delta S > 5$) in two fields

At first sight it is surprising that there is so little difference in distribution between the two populations. It might find an explanation in the fact that in the fields above 6° latitude the stars considered all lie at distances z of more than 1 kpc from the galactic plane. In the central region rather high Z-velocities are required to reach such distances. In fact, the observed density distribution corresponds to a mean square Z-velocity of about 130 km/s (cf. Section 11). This is roughly 4 times the values for high-metal-content variables near the Sun (Oort, 1965), and indicates that also the shorter-period variables in the central bulge may in reality belong to the low-metal-content class.

The similarity in the distribution of the two groups in which we have divided the variables leads one indeed to suspect that they all belong to the same population, and that, *for these stars*, the division into different ranges of period and amplitude does not give a segregation according to age or metal content. The case might be similar to that of globular clusters in which short- and long-period RR Lyrae variables are found side by side.

7. Distribution of Space Density along the Line of Sight

In this section we attempt to derive the distribution of space density which best represents the magnitude distributions given in Fig. 2. We started with what seemed the simplest possible model, consisting of spheroidal equidensity surfaces with equal axial ratios c/a. The density, ν, was assumed to vary as $\nu_{1.5}a^{-\alpha}$, α being again constant; $\nu_{1.5}$ is the density at $a = 1.5$ kpc.

It appeared that these simplest assumptions could in general give an adequate representation of the observations, so that there was no justification for introducing more parameters for the density distribution than the three mentioned: c/a, α and $\nu_{1.5}$, plus the distance of the centre, R_0. There is, however, a fifth unknown quantity, viz. the mean random error of the average magnitude corrected for absorption, ε_{m_0}. Because the

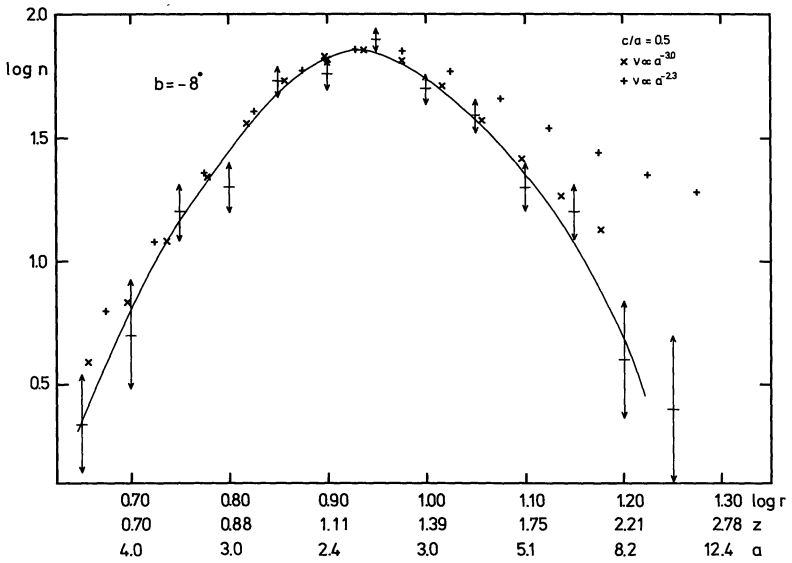

Fig. 4. Comparison of two density distributions with observations in the field at $b=-8°$. Assumed: $c/a=0.5$, $\varepsilon=\pm 0^m.26$. For each distance r the distance from the galactic plane and the semi-major axis of the equidensity surface passing through the point concerned are indicated at the bottom (unit 1 kpc)

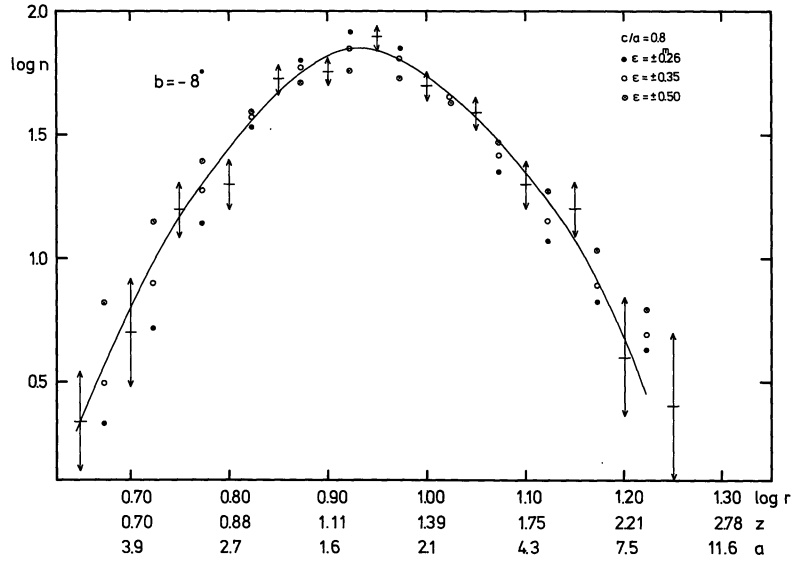

Fig. 5. Illustration of the influence of the assumed random errors. Field at $b=-8°$; c/a was taken 0.8, and $\nu \propto a^{-3.0}$, in all three cases. For each distance r the distance from the galactic plane and the semi-major axis of the equidensity surface passing through the point concerned are indicated at the bottom (unit 1 kpc)

quantities we actually discuss are the distance moduli the dispersion in the true mean absolute magnitudes is supposed to be included in ε_{m_0}; it does not, however, contribute significantly. ε_{m_0} may differ from one field to another, because of differences in the unevenness of the absorption.

In the following figures we represent the observations by the logarithms of the numbers observed per interval of $0^m.25$ as functions of m, and compute corresponding distributions for various values of the parameters mentioned. The shape of the computed curve will depend only on c/a, α and ε_{m_0}. The absolute value of the density and of R_0 are obtained by shifting the calculated curve in vertical and horizontal directions so as to obtain the best fit with the observed curve.

From preliminary analyses we found that a suitable range of the parameters would be covered by the following values: 1.0, 0.8 and 0.5 for c/a; -2.3, -3.0 and -3.6 for α, and $\pm 0^m.26$, $\pm 0^m.35$ and $\pm 0^m.50$ for ε_{m_0}. These have been used in the present section. The lowest value of ε_{m_0} is more or less dictated by the known observational errors.

We start by discussing the *shapes* of the distribution, with a view to determining α, c/a and ε. For this purpose

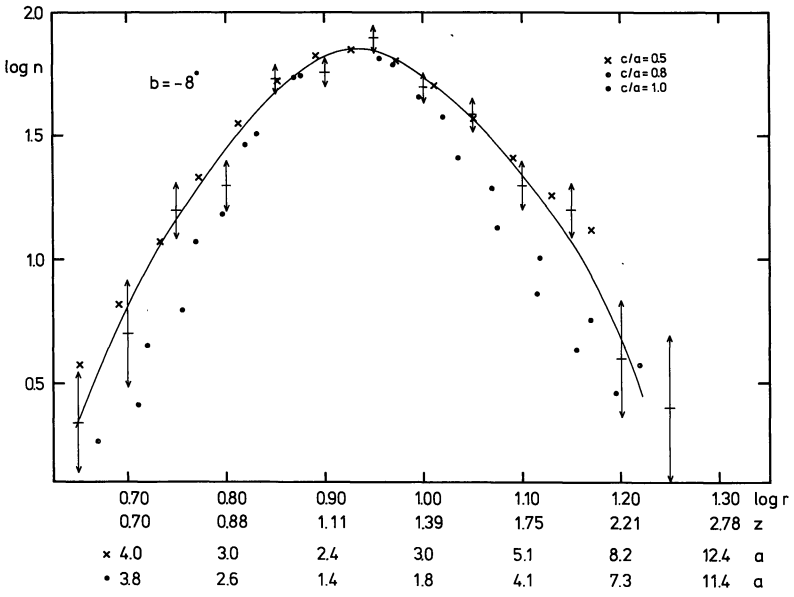

Fig. 6. Effect of the axial ratio on the computed distributions. Field at $b = -8°$, $\nu \propto a^{-3.0}$, $\varepsilon = \pm 0^m.26$. For each distance r the distance from the galactic plane and the semi-major axes of the equidensity surfaces with $c/a = 0.5$ and $c/a = 1$ passing through the point concerned are indicated at the bottom (unit 1 kpc)

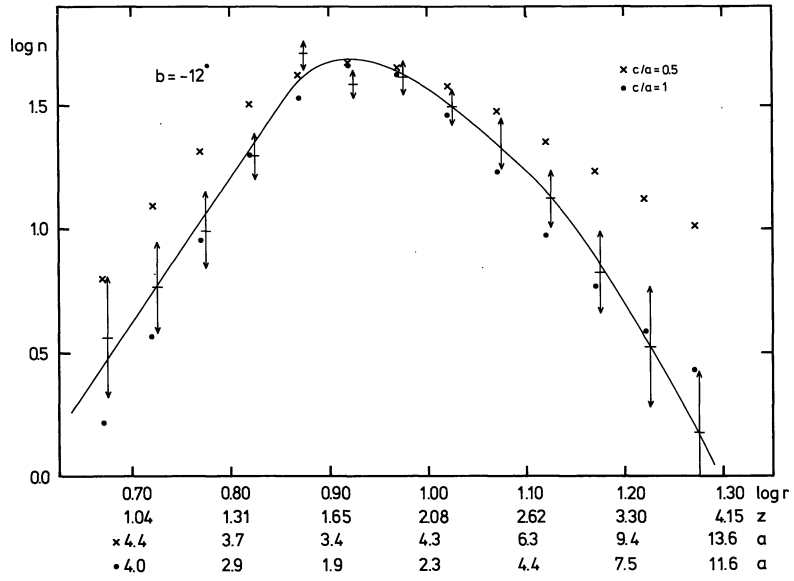

Fig. 7. Field at $b = -12°$. Comparison of observations with the computed numbers for two different axial ratios. $\nu \propto a^{-3.0}$, $\varepsilon = \pm 0^m.26$. For each distance r the distance from the galactic plane and the semi-major axes of the equidensity surfaces with $c/a = 0.5$ and $c/a = 1$ passing through the point concerned are indicated at the bottom (unit 1 kpc)

the maximum of the calculated distribution $\log n_c$ has in each figure been adjusted to coincide, in both co-ordinates, with the maximum of the observed curve.

Co-ordinates are always $\log r$, where r is the distance from the Sun in kpc as computed from $\bar{m}_{pg}$ and $\bar{M}_{pg} = = 0.70$ (taking account of the absorptions given in Table 1), and $\log n_{obs}$, n_{obs} being the number of variables per $0^m.25$ interval in the field considered. The values of a and z which are also indicated are based on the finally adopted distance of 8.73 kpc of the galactic centre.

If the discoveries were complete, and there were no random errors, n should be proportional to r^3 and inversely proportional to a^α. In the computations r and a were expressed in R_0 as a unit. If we denote the values in this unit by $\tilde{r}$ and $\tilde{a}$, $\tilde{a}$ can be found from

$$\tilde{a} = [\tilde{r}^2 \{\cos^2 b + (a/c)^2 \sin^2 b\} - 2\tilde{r} \cos b + 1]^{\frac{1}{2}}. \quad (1)$$

This is the relation for zero longitude. Appropriate, small corrections to take account of a deviating longitude have been applied for field 2 "high" at $l = 4°$, $b = +14°$. The stars were always assumed to lie

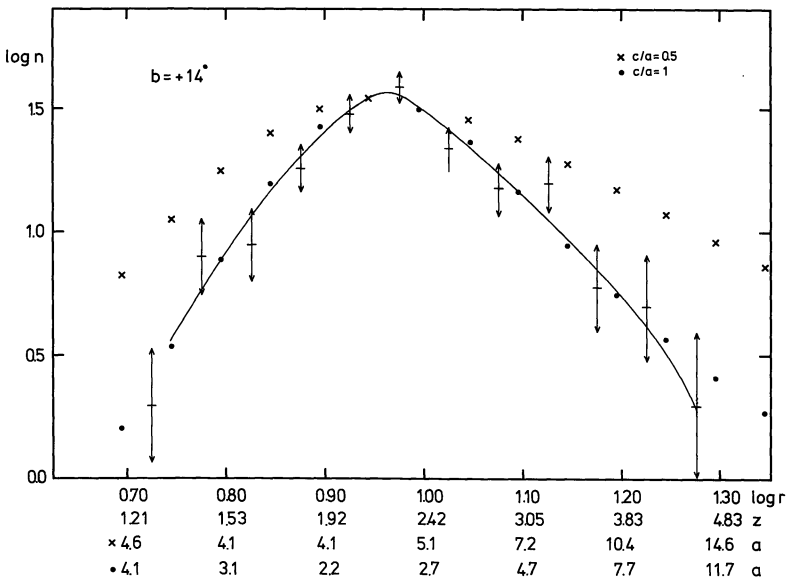

Fig. 8. Field at $b = +14°$. Same legend as Fig. 7

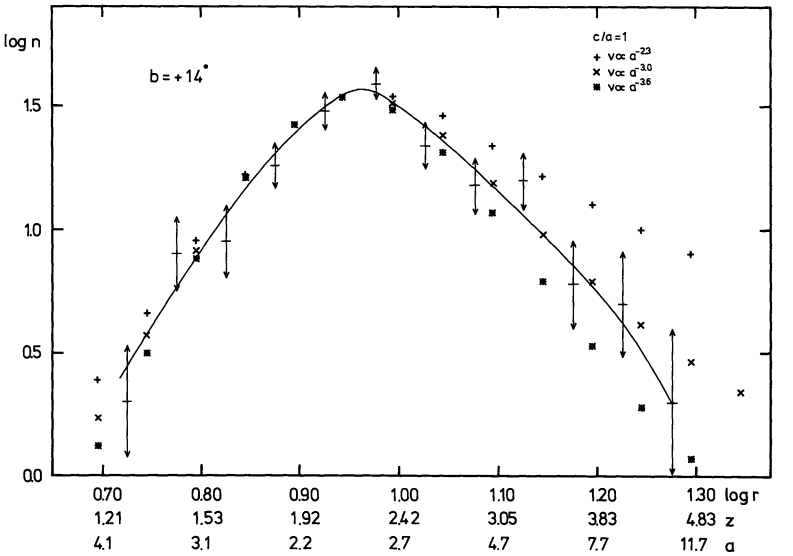

Fig. 9. Comparison between computed numbers for different values of the exponent α in $v \propto a^{\alpha}$. Field at $b = +14°$, $c/a = 1$, $\varepsilon = \pm 0^{m}.26$. For each distance r the distance from the galactic plane and the semi-major axis of the equidensity surface passing through the point concerned are indicated at the bottom (unit 1 kpc)

at the centre of the field. The error introduced by neglecting the spread in position should be inappreciable.

For the comparison with the observed curves the computed distribution of $\log\tilde{r}$ (viz. the distributions of $\tilde{r}^3\tilde{a}^{-\alpha}$) were first convolved with a gaussian error distribution with standard error $\varepsilon_{\log r}(=\frac{1}{5}\varepsilon_{m_0})$, and then divided by the incompleteness factors f read from Fig. 1. The numbers thus arrived at are called "computed", or n_c, and have been used in the following figures.

In practice the parameters c/a and ε cannot be determined independently from the $\log r$ distribution. An increase in the flattening of the equidensity surfaces and an increase in the mean error of the distance moduli both produce an approximately symmetrical widening of the distribution. As a consequence we can only determine lower limits for c/a, which are obtained by using the minimum values of ε based on the directly estimated errors in the magnitudes and the probable dispersion in $\bar{M}$ (cf. Section 5). This minimum is unlikely to be smaller than $\pm 0^{m}.2$. In most cases a value of $\pm 0^{m}.26$ has been used.

The exponent α can be determined unambiguously, from the asymmetry of the curves (cf. Figs. 4 and 9).

In Figs. 4—11, which give a sample of the comparisons made, smooth curves have been drawn through the observed points. These latter are indicated by a

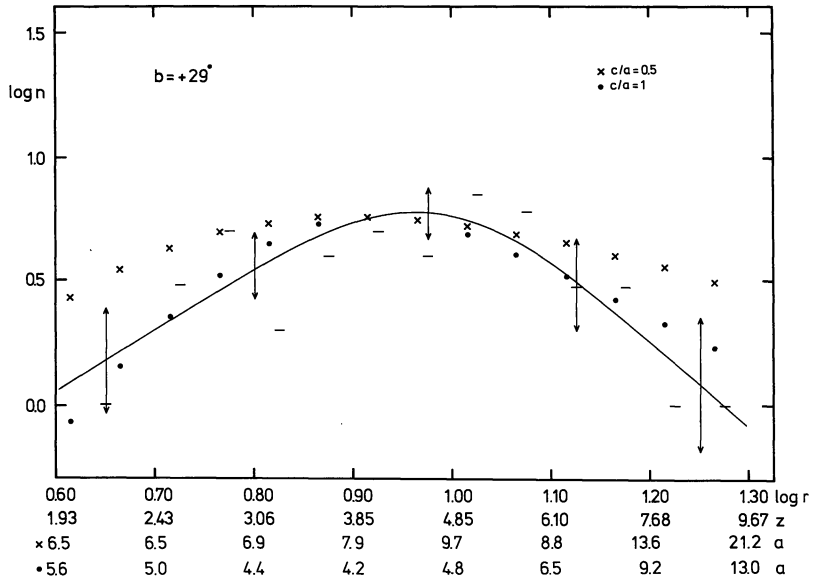

Fig. 10. Field at $b = +29°$. Comparison of observations with numbers computed for $c/a = 1$ and $c/a = 0.5$; $v \propto a^{-3.0}$, $\varepsilon = \pm 0^m.26$. Because of the small number of variables the statistical errors were not indicated for each individual point, but for five supposedly independent parts of the smooth curve by which the observations have been represented. They are shown by vertical lines with double arrows. The observed values have been indicated by horizontal dashes. For each distance r the distance from the galactic plane and the semi-major axes of the equidensity surfaces with $c/a = 0.5$ and $c/a = 1$ passing through the point concerned are indicated at the bottom (unit 1 kpc)

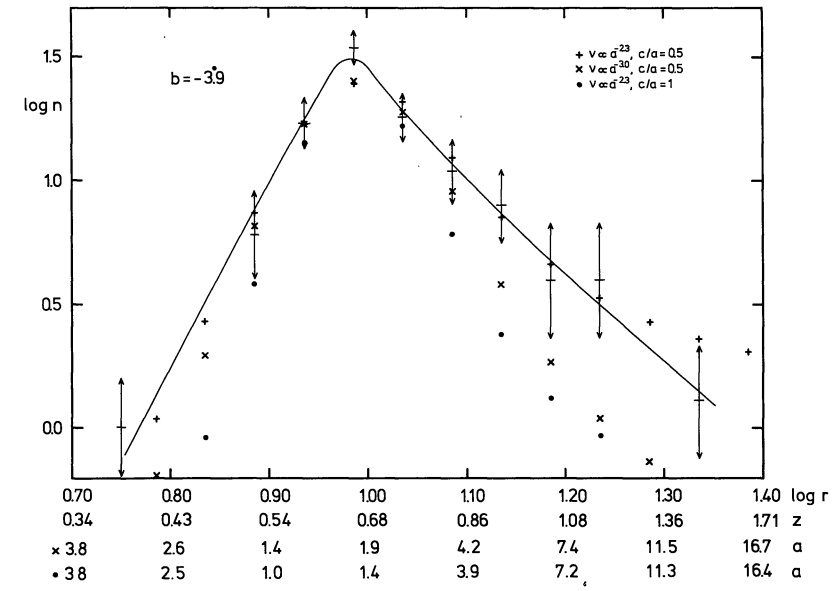

Fig. 11. Field at $b = -3°.9$. Comparisons for $v \propto a^{-2.3}$, $c/a = 1$ and $c/a = 0.5$, and for $v \propto a^{-3.0}$, $c/a = 0.5$. In all cases ε was assumed to be $\pm 0^m.20$. For each distance r the distance from the galactic plane and the semi-major axes of the equidensity surfaces with $c/a = 0.5$ and $c/a = 1$ passing through the point concerned are indicated at the bottom (unit 1 kpc)

horizontal dash and a vertical line extending to either side over a distance equal to the statistical mean error.

We consider first the variation of the density with a. Figures 4 and 9, for $b = -8°$ and $b = +14°$, show that a good representation of the observations can be obtained if $v \propto a^{-3.0}$, while this cannot be adequately done with $v \propto a^{-2.3}$. A similar conclusion holds for $b = -12°$. Only in the low-latitude field ($b = -3°.9$) the density variation is found to be less steep, and the best fit is given by a power of approximately -2.3.

An independent determination of the density variation can be obtained by comparing the maximum densities in the different fields. This shows that the density

decrease along the z-axis, perpendicular to the galactic plane, can also be best represented by an inverse third power of the distance from the centre (cf. Fig. 12).
We have therefore provisionally adopted this power law for the entire central region except for the layer within 1 kpc from the galactic plane where the variation appears to be less steep.
As may be seen from the values of a and z indicated in the figures the above result applies to a region extending to about 5 kpc from the centre in both co-ordinates. The uncertainty in the exponent is estimated at about ± 0.1.

8. Axial Ratio of Equidensity Surfaces

As stated above this quantity is interwoven with the partly unknown mean random error ε. It is quite unlikely that ε would be smaller than $\pm 0^{m}.2$. Most of the calculations were started with an assumed value of $\pm 0^{m}.26$. In two cases ($b=-12°$ and $b=-3°.9$) they were also made with $\varepsilon=\pm 0^{m}.20$. Taking $\alpha=-3.0$ for the fields between 8° and 29°, as argued above, we have found the following results for c/a. For Baade's field at $-3°.9$ α was taken -2.3. Most of the results can be verified from Figs. 4—11.

Table 5. Axial ratio of isodensity surfaces

Field	b	ε	c/a
Baade	− 3°.9	$0^{m}.20$	0.5[a])
3 low	− 8	0.26	0.55
3 low	− 8	0.35	0.8
3 low	− 8	0.50	1
3 high	−12	0.26	0.85
3 high	−12	0.20	0.80
2 high	+14	0.26	1.0
1	+29	0.26	1

[a]) Except for the region within about 1.2 kpc from the centre, where the distributions seem to be nearly spherical.

The fields at −12°, +14° and +29° yield remarkably small flattenings. Axial ratios as low as 0.5 give distributions which deviate widely from the observed curves; the deviations are far larger than the uncertainty in the observations (cf. Figs. 7 and 8). It would not seem possible to decrease the values of c/a very appreciably by assuming still lower values for ε.
For the field at −8° the ratio is indeterminate, because we do not know ε. It may very well be that in this field the variations of the absorption are larger than in the fields at higher latitude, and that as a consequence ε is larger, and that the true axial ratio is the same as in the higher-latitude fields. But it is also possible that the almost spherical distribution holds only for stars beyond $z\sim 1.5$ kpc. Figure 6 shows some comparisons.
From the well-defined data at −12° and +14° we conclude provisionally that c/a lies between 0.8 and 1.0 for the regions concerned.

This result is somewhat surprising in view of the central "bulges" in other spirals, which generally show outspoken flattening. A good example is the nearly edge-on system NGC 4594, where Van Houten (1961) found $c/a=0.55$ for the region within 10 kpc from the centre, and 0.60 for the halo outside 20 kpc. In M 31 the distinction between bulge and disk is more difficult; it is only in the regions closest to the centre that the population-II light sufficiently exceeds the disk light to get a trustworthy picture of the former. Kinman's (1965) data on the axial ratio of the isophotes show that c/a varies from 0.8 close to the centre to about 0.6 near $a=400''$, or 1.5 kpc.
It seems unlikely that the apparent discrepancy between the flattening of the central bulges in external galaxies and the near-sphericity of the distribution of the variables could be due to some error in the latter. For it follows almost directly from the narrowness of the magnitude distributions, which is one of the most striking results of the present survey. All plausible types of errors would tend to make the observed distributions too wide rather than too narrow.
It may be that our RR Lyrae variables are a population which differs kinematically from the population producing the light of the central bulges.
For the field at $-3°.9$ the circumstances are different. The sharpness of the top part of the observed curve indicates that ε cannot be much larger than $\pm 0^{m}.20$; with this value for ε a considerable flattening is found for the bulk of this region between a about 3 kpc on our side of the centre and 6 kpc beyond the centre. Only the very central part seems to be roughly spherical, and to have an excess density (cf. Figs. 11 and 12).

9. Space Densities along the Rotation Axis of the Galaxy

If there are no errors in the distance moduli the relation between the observed numbers per $0^{m}.25$ interval and the space densities per kpc^3 is

$$n_{obs}=3.51\times 10^{-5}\, s v r^3/f, \qquad (2)$$

where f is again the incompleteness factor and s the area of the field in square degrees. If v is proportional to a^{-3} (2) can be written

$$n_{obs}=3.51\times 10^{-5}\, s\,\frac{(r^3/a^3)}{f}\,v a^3,$$

where va^3 is a constant, and $\dfrac{(r^3/a^3)}{f}=\dfrac{(\tilde{r}^3/\tilde{a}^3)}{f}$ is what we have used as computed density. In reality n_{obs} is affected by random errors in the distance moduli, and we have convolved the quantity $\tilde{r}^3/\tilde{a}^3$ by the same error distribution to obtain n_{comp}. The relation is then

$$n_{obs}=3.51\times 10^{-5}\, s n_{comp} v a^3. \qquad (3)$$

Table 6. Space densities along the rotation axis

b	c_m (kpc)	$\log c_m$ (kpc)	$\log \nu_m$ (kpc^{-3})	$\bar{m}_{pg}$
− 3.9	0.59	−0.226	4.06	17.2
− 8	1.27	+0.105	2.52	16.2
−12	1.82	0.261	2.19	15.9
+14	2.27	0.356	2.02	16.5
+29	4.90	0.690	0.71	16.2

We have used (3) to determine the space densities ν_m around the maxima of the observed distributions. The density distribution near the maxima can always be adequately represented by the inverse-cube law. The results are given in Table 6 and Fig. 12. Because the axis directly connected with the maximum is c rather than a, the data are given as functions of c; c_m is the semi-axis of the equidensity surface passing through the maximum of the distribution. The last column of the table gives the mean magnitude at this maximum. It illustrates again how far the most important part of the distribution curve lies above our limiting magnitude of 19.5–20.0.

In Fig. 12 the three density laws considered in the representation of the distributions along the line of sight have been indicated. The a^{-3} variation gives a reasonable representation of the observed points, except for the field nearest to the centre, in which the density is 2.6 times higher than given by the a^{-3} law. An excess at the same place had already been noted in the density distribution along the line of sight, but of smaller size. The deviations at $b=-8°$ and $b=+14°$ are no larger than would be expected from the uncertainty in ε and in the absorption. For example: if we take $\varepsilon=\pm 0^m.50$ instead of $\pm 0^m.35$ for $b=-8°$ the deviation in $\log \nu$ is reduced from -0.13 to -0.04. A variation with $a^{-3.6}$, however, would make the residuals for $b=-8°$ and $+14°$ less plausible. An $a^{-2.3}$ variation gives improbably large deviations at $b=-3°.9$ and $b=+29°$.

We have therefore provisionally adopted the r^{-3} law for the density variation along the rotation axis. This variation is the same as found in Section 7, and thus applies to both cylindrical co-ordinates ω and z, with the exception of the region of Baade's field, i.e., below z about 1 kpc. As may be seen from an inspection of Figs. 4—12 the density variation has been fairly well observed over a spherical volume of about 5 kpc radius around the centre. The best determined part lies between 1 and 3 kpc from the centre. From Fig. 12 the absolute density at $R=1.5$ kpc is estimated as $\nu_{1.5}=260$ per kpc^3. At other points it is $\nu(R)=260\,(1.5/R)^3$, except in the galactic layer.

If we extrapolate this expression to the distance of the Sun we obtain 1.3 per kpc^3. Assuming that the RR Lyrae variables within 1 kpc are completely known the observed density of the a- and b-types around the Sun is found to be 8.4 per kpc^3. For the volume within 0.75 kpc the density would be 10.7. These densities are larger than that found from the R^{-3} law, but this is not surprising since the latter refers to pure halo objects, while we are comparing with a region near the galactic plane. An extrapolation from the results obtained in Baade's field, with $c/a=0.5$ and $\nu \propto a^{-2.3}$, gives $\nu=35$ near the Sun, deviating in the opposite direction from the observed density. One may conclude that the local density does not conflict with the data for the inner region.

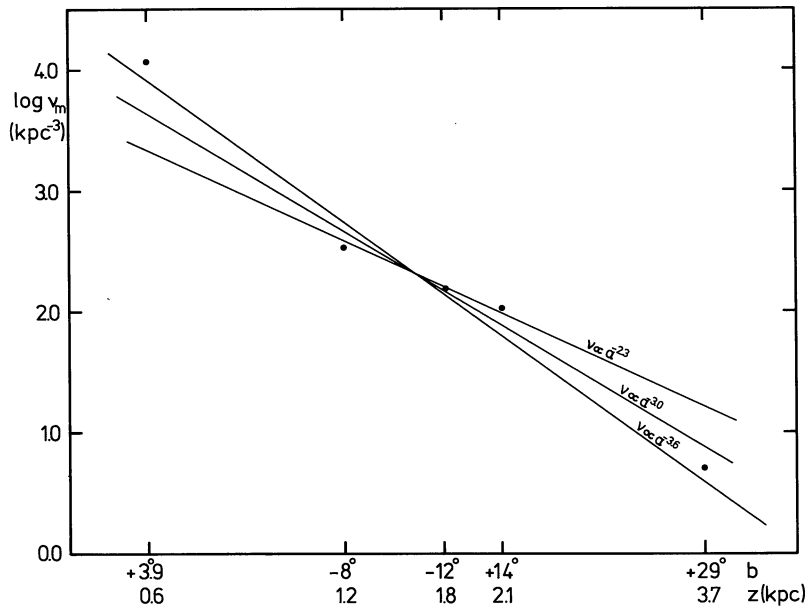

Fig. 12. Density distribution perpendicular to the galactic plane

10. The Distance of the Centre

The superposition of the computed log$n$ curves which gave the best fits to the observed distributions of log$n$ yields at once the values of R_0. For the abscissa of the computed curves are log (r/R_0), while those of the observed curves are log$r$, as found from the apparent magnitude and the assumed values of $\bar{M}_{pg}$ and A_{pg}.
The results are given in Table 7.
The weights are of necessity somewhat arbitrary. They rest on the numbers of stars in the various fields, the widths of the distributions (both given in Table 1) and an estimate of the uncertainty in the assumed absorptions. But for this last factor there would have been greater differences in weight.
The weighted mean is $R_0 = 8.73$, with a mean error of ± 0.23 as estimated from the residuals of the individual fields. The residuals do not seem to be larger than might be caused by the uncertainty of the absorptions. The changes in the latter which would be required to bring the values of R_0 into exact agreement are indicated under ΔA_{pg}. But there are of course other errors as well. The principal uncertainty, however, is in the assumed value of $\bar{M}_{pg}$, which was estimated in Section 2 to be about ± 0.15, corresponding to ± 0.6 in R_0.

Table 7. Determination of the distance to the centre

b	R_0 (kpc)	Weight	ΔA_{pg}
− 3°.9	9.50	1	+0^m.19
− 8	8.41	1	−0.08
−12	8.41	2/3	−0.08
+14	8.81	2/3	+0.02
+29	7.3	1/5	—

Comparison with other Determinations

Van den Bergh (1974; see also Van den Bergh and Herbst, 1974) has recently made an original attempt to determine R_0 from the sharp increase in faint stars between 19^m and 20^m in a field near the centre of our "field 3 low", observed with the Hale 200-inch telescope. On the supposition that the stars near his maximum would be main-sequence stars at the turn-off point in the main-sequence of population II Van den Bergh derives $R_0 = 9.2 \pm 2.2$ kpc. The assumption that the stars near the maximum lie at this break-off point is rather arbitrary, however. In a cluster like M 3 the luminosity function of the main-sequence stars rises by a factor of roughly 2 over the first magnitude beyond the turn-off point, and only flattens off between 1^m.5 and 2^m.0 beyond this point. It may therefore be just as well assumed that the maximum in Van den Bergh's curve corresponds to stars 1^m beyond the turn-off point, in which case the distance would be reduced correspondingly.

The distance of the centre can, in principle, also be determined by measuring the distance to stars of which one can assume on the basis of their motions that they lie at about the same distance from the centre as the Sun. Various attempts have been made to find R_0 in this way, most recently and most completely by Balona and Feast (1974) from distant O and B stars. They obtain $R_0 = 9.0$ kpc, "with a range of about 7.7 to 10.9 kpc". The method is not very sensitive. For if one wants to determine R_0 from OB stars independently of the determination of the constant A the method consists essentially in finding the longitude l_0 at which stars at a given average distance, in the case of Balona and Feast 2.5 or 3.0 kpc, have zero radial velocity. This longitude changes only 1°.5 if R_0 is changed by 1 kpc. It is doubtful whether the available data allow an accuracy of better than a few degrees. Still more serious is the effect of systematic streamings connected with the spiral wave. A rough estimate indicates that these could cause errors of the order of 30% in R_0.

11. The Velocity Distribution of the Variables in the Central Region

From rotation velocities in the nuclear disk, and an interpolation between the outer limit of this disk at $R = 0.8$ kpc and the rotations measured at distances beyond 3 kpc, a rough estimate can be made of the potential field in the region discussed in the present article. The estimates are given in Table 8 in units of $M_\odot$, pc, and 30 km/s for v. In these units the constant of gravitation is equal to 1. In order to get a rough idea of the velocity distribution required to produce the R^{-3} variation of the density and its near-isotropic distribution we have assumed the potential to be spherically symmetrical between $R = 0.6$ and 3.0 kpc. The R^{-3} law is found to correspond to a practically Maxwellian velocity distribution, with a dispersion of roughly 125 km/s in each co-ordinate. In the case of a Maxwellian velocity distribution the relation between v and Φ is

$$\frac{v(R)}{v(o)} = e^{-\frac{\Phi(R)-\Phi(o)}{\langle v_x^2\rangle}},$$

or

$$\log \frac{v(R)}{v(o)} = -\frac{\mathrm{Mod}\,\{\Phi(R)-\Phi(o)\}}{\langle v_x^2\rangle}. \qquad (4)$$

Table 8. Gravitational potential and velocity distribution

R (pc)	$\Phi(R)-\Phi(o)$ (30 km/s)^2	$\Phi(R)-\Phi(500)$ (30 km/s)^2	$\log \frac{v(R)}{v(500)}$	disp v_x (km/s)
50	125			
500	255			
1000	294	39	0.903	130
2000	328	73	1.806	126
3000	342	87	2.334	121

The fourth column of the table gives $\Delta \log v$ corresponding to the R^{-3} variation. The velocity dispersions computed from formula (4) are shown in the last column. The range from $R = 0.5$ to 3.0 kpc can be fairly represented by the *same* dispersion, of 4.2 units, or 125 km/s.

Using the *same* velocity dispersion to extrapolate inward we get a density at 50 pc which is 1600 times that at 500 pc, the density would therefore continue to increase roughly as R^{-3}.

It may be noted that in the region with which we are concerned the total *mass* density varies with a much lower power of R; it is roughly proportional to $R^{-1.3}$.

The velocity dispersion of these stars is remarkably similar to the average dispersion for the metal-poor RR Lyrae variables in the solar neighbourhood. According to a table given in Stars and Stellar Systems, Vol. V (Oort, 1965), this average is 140 km/s, with an estimated mean error of ± 20, but the distribution of the velocities is strongly elongated in the radial direction.

12. Compatibility with the Data on Galactic Rotation, and Rediscussion of the Rotation Constants

It remains to investigate whether the relatively low value we have found for R_0 is compatible with existing data on galactic rotation. These data give information on R_0 in two ways, viz., by the product AR_0 found from 21-cm line observations, and through the value of Θ_0/R_0 derived from the constants of differential rotation.

We first sum up what appear to be the best present values of the constants A and B.

A. In Table 9 are collected the most significant results for A. The determinations listed are largely independent as far as the calibration of the distances is concerned, but the first four are *not* entirely independent in that they may be affected by similar local "streams". The four types of objects differ in age, however, and will not, therefore, be affected in exactly the same manner. The proper-motion result is derived from motions of faint stars in the McCormick and Cape catalogues, which are much older; moreover, the transverse motions are affected quite differently. However, as these stars are about two times nearer than those in the other groups, the influence of local streams will be more serious. For the cepheids Kraft and Schmidt gave a value of 15, based on a calibration of their absolute magnitudes with the aid of 5 cepheids in galactic clusters. They stated that an independent calibration by means of proper motions gave 1.27 times lower distances, which would lead to $A = 19$. For our purpose of combining independent determinations we prefer this latter result because it is independent of the calibrations for the OB stars and the clusters.

Table 9. Determinations of the constant A

Type of stars	A	(m.e.)	Weight	Ref.
O and B	16.8	± 0.6	2	Balona and Feast (1974)
Optical interstellar lines	18.1	± 0.7	1.5	Balona and Feast (1974)
Cepheids	19		1.5	Kraft and Schmidt (1963)[a])
Galactic clusters	15	± 3	1	Johnson and Svolopoulos (1961)
Proper motions of 9th mag stars	15.5	± 1.9	2	Fricke (1967)

[a]) The authors themselves concluded that the best value from cepheids would be 15, as based on absolute magnitudes derived from 5 cepheids in clusters. However, because this value depends on the distance scale for the clusters, which is used in the next line, we have preferred for the present overview the independent calibration by means of proper motions. According to the authors this would give 1.27 times lower distances and, therefore, $A = 19$. Had we adopted 15 instead the total average would have become 16.2.

The mean errors are those given by the investigators. They do not include the uncertainty of the calibration. An error of $\pm 0^{m}.2$ in the adopted absolute magnitudes of the O and B stars corresponds to an error of 9.5%, or ± 1.6 km/s · kpc, in the tabulated value of A.

In combining the five results we assigned the relative weights shown in the table. The clusters were given a smaller weight because of their small number. The weighted mean is

$$A = 16.9 \text{ km/s} \cdot \text{kpc} \pm 0.9 \text{ (m.e.)}.$$

In a recent publication Crézé (1973) has shown that the value of A would be increased by about 1 km/s · kpc if due account is taken of the bias caused by random errors. The effect was taken into account by Balona and Feast, but will have affected the cepheids and the clusters. For the present we have neglected it, and have adopted the value of 16.9.

Lin *et al.* (1974) have calculated what consequence the systematic motions accompanying the spiral structure have for the determination of A from stars at distances of 1, 2 and 3 kpc respectively. They find that these streams have not seriously affected the constants A and B.

B. The only direct way in which the constant B can be determined is from proper motions. But its smallness (about $0''.002$ per annum) and the probable superposition of systematic streams makes this determination liable to considerable uncertainty. We consider that the indirect determination from the ratio of the two axes a and b of the velocity ellipsoid that lie in the galactic plane is more reliable, although here also there are systematic errors due to local effects. That such effects exist is evident from the deviation of the vertex. As this deviation is largest for the youngest stars, as well as for the nearest stars, we limit our discussion to the G, K and M giants, but even they show a very appreciable vertex deviation. Delhaye (1965) lists the following values for b/a: 0.69, 0.68, 0.68 and 0.74 for G, K 0, K 3

and M giants respectively; the average is 0.69. A result which may be more representative for a larger part of the galactic plane has been obtained by Hins and Blaauw (1948) from the proper motions of faint stars in Kapteyn's Selected Areas and in regions measured at the McCormick Observatory. They found $b/a = 0.49 \pm 0.04$ (m.e.). Schmidt (1965) has critized their use of mean parallaxes correlated with star counts, and suggested that this has caused a systematic error in the very low axial ratio of 0.39 found from the Selected Area stars. With Schmidt's alternative, rather extreme, assumption that the parallaxes would be independent of the star counts the ratio is raised to 0.52. We adopt the average of the two results, 0.46. In the case of the McCormick motions the parallax problem can be avoided by using the ratios between the dispersions in longitude and those in latitude. This yields $b/a = 0.54 \pm 0.06$ (m.e.). Taking Blaauw and Hins' other, less certain, solutions also into account we may put the final average from faint stars at 0.54 ± 0.05.

The relation

$$\frac{-B}{A-B} = \frac{b^2}{a^2}$$

then yields $B = -7.0 \pm 1.8$ (m.e.), if we take $A = 16.9$ as derived above. The axial ratio 0.69 found from the bright stars leads to $B = -15.4$, but because of the considerable vertex deviation this should be considered as much more uncertain.

The direct determination from proper motions, of which we believe the most significant is again that made by Fricke (1967) from faint stars, gives -7.6 ± 1.4 (m.e.). We prefer this value to the one Fricke derived from bright stars, because the latter are again likely to be more disturbed by local streams. Two other interesting results have been obtained from proper motions measured relative to galaxies by Fatchikhin (1970) and by Vasilevskis and Klemola (1971). They are $B = -10.4 \pm 4.1$ and -12.5 ± 4.1, respectively. They are independent of the usual fundamental system. Giving the average of these two half of the weight of Fricke's result we adopt $B = -8.9 \pm 1.5$ as the total average of the direct determinations. This compares well enough with the values found from the ellipsoidal velocity distribution. We have finally adopted $B = -9.0$ km/s · kpc, with an estimated mean error of ± 1.5.

We next consider the circular velocity near the Sun, Θ_0. The only direct information we have on Θ_0 is that it cannot be less than the velocity of the local standard of rest relative to the most extreme halo population. The extreme subdwarfs and RR Lyrae variables with lowest metal content yield velocities of 183 ± 19 and 220 ± 23 km/s, respectively, computed from space motions; from *radial* velocities of 123 RR Lyrae variables of the same population van Herk found 168 ± 9 km/s (m.e.) (cf. *Stars and Stellar Systems*, Vol. V; Oort, Table 5, 1965). Because even these extreme halo stars will presumably have *some* angular momentum, it may be concluded that

$$\Theta_0 > 200 \text{ km/s}.$$

This can be translated into a lower limit for R_0 by the relation $\Theta_0/R_0 = A - B = 25.9$ km/s · kpc ± 2.2 (m.e.), according to the above results for A and B. We thus find

$$R_0 > 7.7 \text{ kpc} \pm 0.7 \text{ (m.e.)},$$

which is evidently compatible with the result from the RR Lyrae variables in Section 10. The value of $8.7 \text{ kpc} \pm 0.6$, derived there, would correspond with $\Theta_0 = 226 \text{ km/s} \pm 27$ (m.e.).

It should be pointed out that a decrease of the rotation velocity below the standard value of 250 km/s leads to a nearly equal increase of the velocity at which the Andromeda nebula and the Galactic System approach each other. This, in turn, would lead to a further increase of the already very high extra mass in the Local Group required to explain the 100 km/s approach velocity derived with $\Theta_0 = 250$ km/s (cf. Kahn and Woltjer, 1959; Oort, 1970).

Finally, we must discuss the determination of the quantity AR_0 from 21-cm observations. In his article in Vol. V of *Stars and Stellar Systems*, Schmidt (1965) concluded that AR_0 would lie between 135 and 150 km/s. These values were derived from the "terminal" velocities observed in longitudes where the rotation curve showed secondary maxima, which Schmidt interpreted as a sign that the line of sight passed through a spiral arm at the tangent point. Subsequent studies (cf. for instance Burton and Shane, 1970) have shown, however, that these secondary maxima are caused by the stream motions connected with the spiral arms. The terminal velocities in these directions are therefore too high. However, the "basic" rotation curve used by these authors is also higher than that used by Schmidt. The uncertainty—as indicated for instance by the discrepancy between the rotation curves on the two sides of the centre—remains considerable, and we can at present claim no more than that AR_0 lies between about 120 and 150 km/s.

With $A = 16.9$ this corresponds to a range in R_0 from 7.1 to 8.9 kpc, which agrees sufficiently with the value 8.7 kpc derived in the present article.

Summarizing we conclude that our somewhat lower distance to the centre than the standard value of 10 kpc, shows no important discrepancies when compared to the existing data on the galactic rotation. To avoid confusion it may, however, be recommendable for the present to continue using the standard values of 10 kpc for R_0 and 250 km/s for Θ_0, except in special cases.

Acknowledgements. We thank Sidney van den Bergh for drawing our attention to a serious error in the first preprint version of the article, Maarten Schmidt for suggesting an extension of the discussion which has proved to be quite fertile, Tjeerd van Albada for a comparison with his independent calculations, Georg Comello for preparing the drawings.

References

Balona, L. A., Feast, M. W. 1974, *Monthly Notices Roy. Astron. Soc.* **167**, 621

Bergh, S. van den 1971, *Astron. J.* **76**, 1082

Bergh, S. van den 1974, *Astrophys. J.* **188**, L 9

Bergh, S. van den, Herbst, E. 1974, *Astron. J.* **79**, 603

Burton, W. B., Shane, W. W. 1970, The Spiral Structure of our Galaxy, Eds. F. Becker and G. Contopoulos, p. 397

Clube, S. V. M., Evans, D. S., Jones, D. H. P. 1969, *Mem. Roy. Astron. Soc.* **72**, 101

Crézé, M. 1973, *Astron. & Astrophys.* **22**, 85

Delhaye, J. 1965, Stars and Stellar Systems, Vol. V, Eds. A. Blaauw and M. Schmidt, p. 513

Eddington, A. S. 1913, *Monthly Notices Roy. Astron. Soc.* **73**, 359

Fatchikhin, N. V. 1970, *Astron. Z.* **47**, 619 (*Soviet Astron.* **14**, 495)

Fitch, W. S., Wiesniewski, W. L., Johnson, H. L. 1966, *Commun. Lunar Planet. Lab.* **5**, No. 71

Fricke, W. 1967, *Astron. J.* **72**, 642

Graham, J. A. 1973, Proc. I.A.U. Symp. 59

Hemenway, M. K. M. 1971, Thesis, University of Virginia, Charlottesville

Herk, G. van 1965, *Bull. Astron. Inst. Neth.* **18**, 71

Hins, C. J., Blaauw, A. 1948, *Bull. Astron. Inst. Neth.* **10**, 365

Hodge, P. W. 1974, *Astrophys. J.* **192**, 21

Holmberg, E. B. 1974, *Astron. & Astrophys.* **35**, 121

Houten, C. J. van 1961, *Bull. Astron. Inst. Neth.* **16**, 1

Hubble, E. P. 1934, *Astrophys. J.* **79**, 8

Johnson, H. L., Svolopoulos, S. N. 1961, *Astrophys. J.* **134**, 868

Kahn, F. D., Woltjer, L. 1959, *Astrophys. J.* **130**, 705

Kinman, T. D. 1965, *Astrophys. J.* **142**, 1376

Knapp, G. R., Kerr, F. J. 1974, *Astron. & Astrophys.* **35**, 361

Kraft, R. P., Schmidt, M. 1963, *Astrophys. J.* **137**, 249

Lin, C. C., Yuan, Chi, Roberts, W. W. 1974, paper presented at Joint Discussion, I.A.U. General Assembly, Sydney, N.S.W.

Oort, J. H. 1965, Stars and Stellar Systems, Vol. V. Eds. A. Blaauw and M. Schmidt, p. 455

Oort, J. H. 1970, *Astron. & Astrophys.* **7**, 381

Oosterhoff, P. Th., Ponsen, J., Schuurman, M. C. 1967, *Bull. Astron. Inst. Neth. Suppl.* **1**, 397

Oosterhoff, P. Th., Ponsen, J. 1968, *Bull. Astron. Inst. Neth. Suppl.* **3**, 79

Plaut, L. 1966, *Bull. Astron. Inst. Neth. Suppl.* **1**, 105 (Paper I)

Plaut, L. 1968, *Bull. Astron. Inst. Neth. Suppl.* **2**, 293, (Paper II)

Plaut, L. 1968, *Bull. Astron. Inst. Neth. Suppl.* **3**, 1 (Paper III)

Plaut, L. 1970, *Astron. & Astrophys.* **8**, 341 (Paper IV)

Plaut, L. 1971, *Astron. & Astrophys. Suppl. Ser.* **4**, 75 (Paper V)

Plaut, L. 1973a, *Astron. & Astrophys.* **26**, 317

Plaut, L. 1973b, *Astron. & Astrophys. Suppl. Ser.* **12**, 351 (Paper VI)

Sandage, A. R. 1970, *Astrophys. J.* **162**, 841

Schmidt, M. 1965, Stars and Stellar Systems, Vol. V, Eds. A. Blaauw and M. Schmidt, p. 513

Shane, C. D., Wirtanen, C. A. 1967, *Publ. Lick Obs.* **22**, Pt. 1

Vasilevskis, S., Klemola, A. R. 1971, *Astron. J.* **76**, 508

Wesselink, A. J. 1961, *Monthly Notices Roy. Astron. Soc.* **122**, 509

Woolley, R., Harding, G. R., Cassels, A. I., Saunders, J. 1965, *Roy. Obs. Bull.* **97**

J. H. Oort
Sterrewacht, Huygens Laboratorium
Wassenaarseweg 78
Leiden-2405, The Netherlands

L. Plaut
Sterrenkundig Laboratorium "Kapteyn"
Postbus 800
Groningen-8002, The Netherlands